AGU100 ADVANCING EARTH AND SPACE SCIENCE

Earth and Space Science

RESEARCH ARTICLE
10.1029/2018EA000395

Nonlinear Trends and Nonstationary Oscillations as Extracted From Annual Accumulated Precipitation at Mexico City

B. Martinez-Lopez[1], A. I. Quintanar[1], W. D. Cabos-Narvaez[2], C. Gay-Garcia[1], and D. V. Sein[3,4]

[1]Universidad Nacional Autónoma de México, Mexico City, Mexico, [2]Department of Mathematics and Physics, Universidad de Alcalá, Alcalá de Henares, Spain, [3]Alfred-Wegener-Institut Helmholtz-Zentrum für Polar- und Meeresforschung, Bremerhaven, Germany, [4]P. P. Shirshov Institute of Oceanology RAS, Moscow, Russia

Key Points:
- Long-term secular positive precipitation trends in Mexico City cannot be accounted for by man-induced climate change alone
- The Atlantic Multidecadal Oscillation can be explained as an integrated response of the upper ocean to surface stochastic forcing
- Long-term positive trends in precipitation in Mexico City can be thought of as the increasing portion of a longer period oscillation

Supporting Information:
- Supporting Information S1

Correspondence to:
B. Martinez-Lopez,
benmar@atmosfera.unam.mx

Citation:
Martinez-Lopez, B., Quintanar, A. I., Cabos-Narvaez, W. D., Gay-Garcia, C., & Sein, D. V. (2018). Nonlinear trends and nonstationary oscillations as extracted from annual accumulated precipitation at Mexico City. *Earth and Space Science*, *5*. https://doi.org/10.1029/2018EA000395

Received 26 MAR 2018
Accepted 3 AUG 2018
Accepted article online 23 AUG 2018

Abstract Extracted nonstationary oscillations and nonlinear trends of precipitation and sea surface temperature (SST) data reveal that rainfall variability in Mexico City is mainly composed by a long-term positive trend, a multidecadal oscillation highly correlated with the Atlantic Multidecadal Oscillation (AMO), and year-to-year variability. The precipitation trend, lasting for more than a century, cannot be attributed to global warming or urbanization alone; rather, it can be thought of as part of a natural oscillation composed of alternating wet-dry anomalies with a period of a couple of centuries, as past evidence indicates. To further test the dependence of the AMO-related component, yearly SST time series were derived from a simplified model of the atmosphere-ocean system forced by white noise. The simulated SST time series exhibits AMO-like variability entirely consistent with the observed one, implying that North Atlantic SST multidecadal variability can be seen as the integrated response of surface ocean layers to external stochastic atmospheric forcing.

Plain Language Summary In this work, nonlinear trends and nonstationary oscillations are extracted from both annual accumulated precipitation and sea surface temperature (SST) data. Our results show that the precipitation variability in Mexico City is mainly composed by a very long-term positive trend of more than a century, a multidecadal oscillation highly correlated with the Atlantic Multidecadal Oscillation (AMO), and year-to-year variability. The long-term positive trend cannot be caused by global warming or urbanization alone; rather, it can be seen as the positive part of a natural oscillation composed of alternating wet-dry anomalies with a period of a couple of centuries, as there are past evidence supporting this interpretation. In order to get a depth understanding of the origin of the AMO-related component, yearly SST time series were obtained by using a simple box model of the ocean-atmosphere system forced by white noise (short timescale atmospheric forcing). This simple model is able to simulate SST anomalies that exhibit AMO-like variability that is entirely consistent with the observed one, implying that North Atlantic SST multidecadal variability can be seen simply as the response of near-surface layers of the ocean to stochastic atmospheric forcing.

1. Introduction

Mexico City (CDMX) was grounded on what was once a lake surrounded by high mountains. CDMX has an accumulated annual precipitation of more than 1,000 mm over the southwestern part of the city (Jauregui, 1973; Ochoa et al., 2015), which is due to its geographical position and surrounding complex topography. Unfortunately, this large volume of water has been more of a problem than a solution to the increasing water demand because both municipal and federal authorities have been unable to solve the flooding and sewage problems that have affected CDMX for centuries. Clearly, as a result of man-made-induced global warming it is expected that certain regions of the globe will experience larger or lesser evaporation rates and precipitation rates. For this reason, it is quite important for a catchment basin such as the CDMX to acquire the proper research tools that would enable decision makers to plan for future scenarios that may include extreme events resulting of changes in intensity of the hydrological cycle. Therefore, a relevant research issue for the CDMX is to evaluate the change in intensity of the hydrological cycle that could occur over this region under a man-induced global warming of the atmosphere and the oceans.

As stated by Easterling et al. (2000), “One of the major concerns with a potential change in climate is that an increase in extreme events will occur.” Today, almost two decades later, the observed increase in the occurrence of extreme hydrometeorological events across the world has motivated intense debates and discussions about their possible link to global warming (Allan & Soden, 2008; Coumou & Rahmstorf, 2012; Donat et al., 2016; Westra et al., 2014). In particular, in the last few years the residents of CDMX have witnessed a large number of torrential downpours occurring with unusual frequency and intensity and have demanded concrete answers about the cause of the increased rainfall they perceive and, above all, about what the future holds regarding changes in mean precipitation.

Definitive answers are yet to be established regarding the long-term variation in the intensity of the hydrological cycle at global and regional scales; however, some basic statements can be made concerning to precipitation trends and their possible relation to man-made climate change. On a global basis, water vapor increases by about 7% for every degree centigrade of warming because a warmer atmosphere is able to hold more water vapor (Held & Soden, 2006; Trenberth, 2011). How this increasing amount of water vapor translates into changes in both global and regional rainfall is a key open issue. There is observational evidence pointing out that wet regions could become wetter over ocean areas. The case for land, however, is more difficult to assess in such simple terms (Greve & Seneviratne, 2015). In recent years, the evidence indicates that some events of extreme weather are more frequent and that this behavior can be linked to human activities influencing climate (Coumou & Rahmstorf, 2012). These authors conclude: “we review the evidence and argue that for some types of extreme -notably heatwaves, but also precipitation extremes- there is now strong evidence linking specific events or an increase in their numbers to the human influence on climate. For other types of extreme, such as storms, the available evidence is less conclusive, but based on observed trends and basic physical concepts it is nevertheless plausible to expect an increase.”

What should we expect for the CDMX? To start answering this question we must first analyze the historical precipitation records available for the country. While in general there is a shortage of adequate-quality and long-term precipitation data coverage, Central Mexico has the longest time series record of daily accumulated precipitation. At the CDMX, a weather station has operated continuously during the last 100 years. Data from this site were used in this study, as indicated in the next section.

Results of available numerical climate simulations constitute another possible way to get additional information regarding the historic and the future evolution of rainfall in CDMX. The time evolution of rainfall, however, is by far, the most difficult variable to simulate compared to say, temperature (Intergovernmental Panel on Climate Change, 2013). This is due, on the one hand, to the coarse resolution used by general circulation models (GCMs) in climate simulations, and to the deficiency in representing moist processes at these scales, on the other. Note that the size of a typical grid cell of GCMs in CMIP5 was of the order of 1° in the ocean and 100 km in the atmosphere (Taylor et al., 2012). This is, clearly, too coarse to represent mesoscale convective processes, particularly over complex terrain in Mexico. For example, Kumar et al. (2013) evaluated precipitation and temperature trends in CMIP5 twentieth-century climate simulations and showed that almost all of Mexico had experienced decreasing trends of precipitation as indicated by the multimodel-ensemble average. Their analysis of the observations in the historical record, however, indicated an opposite trend. To exploit the potential to add value to coarse model output from GCMs one possible route is to perform dynamical downscaling by running a regional climate model with increased spatial resolution (few tens of kilometers) driven by GCMs output at its lateral boundaries. To the best of our knowledge, not such study has been done with enough spatial resolution to evaluate precipitation trends in Mexico during the twentieth century. Nevertheless, there are reanalysis covering the last decades, together with satellite precipitation data, which can be used to infer precipitation changes over a significant period of time.

Due to its thermal capacity, the ocean stores a huge amount of energy and therefore plays a key part of the climate system. On seasonal and decadal timescales, the ocean memory plays a fundamental role in setting the space and timescales for variability (Latif, 2013). Because the energy fluxes between the ocean and the atmosphere strongly depend on the sea surface temperature (SST) fields (Deser et al., 2010), the SSTs regulate the variability of climate on a wide range of both temporal and spatial scales. Due to Mexico’s geographical location, we can expect moisture transport from the Atlantic and Pacific Oceans to influence the time evolution of the precipitation field in Central Mexico. For example, at interannual timescales, El Niño–Southern Oscillation (ENSO) influences the variability of the precipitation field in northwestern Mexico (Castro et al., 2001; Higgins et al., 1999; Pavia, 2009; Pavia et al., 2016), while at decadal timescales, the North Atlantic Oscillation affects northeastern Mexico (Santillán et al., 2012). The Pacific Decadal Oscillation (PDO) also influences precipitation variability. For example, Pavia et al. (2006) found that ENSO favors wet summer conditions when a negative PDO is present and favors wet winter conditions with a positive PDO. At longer, multidecadal timescales, the AMO plays a significant role on the precipitation variability in Mexico. For example, when the AMO is positive, dry conditions are observed in northwest Mexico (Curtis, 2008). Méndez and Magaña (2010) analyzed further and found that a positive AMO, acting together with a negative PDO, is related to drought conditions in Northern Mexico, while a negative AMO plus a positive PDO are related to drought conditions in Central Mexico–Southern Mexico.

At interannual and longer timescales, the SST variability in the North Atlantic can be seen as a multidecadal oscillation plus a secular warming trend (Knight, 2009). The AMO represents a mode of natural variability in the North Atlantic Ocean, characterized by an alternation of cold and warm SST anomalies every few decades (Kerr, 2000), with an estimated period of about 60–80 years (Delworth et al., 2007; Schlesinger & Ramankutty, 1994), and influencing North American summer rainfall (Enfield et al., 2001; Sutton & Hodson, 2005). The length and consistency of the oscillation cycle, however, remains a topic of considerable debate (Alexander et al., 2014), and even the physical mechanism behind the AMO is not well understood (Clement et al., 2015).

Although an important open key question is how to estimate the effects that any underlying trends or low-frequency variability imprint on evolving regional climates, a fundamental and more daunting problem is how to distinguish between long-term oscillations and time-varying secular trends immersed in a time series (Wu et al., 2011). This problem is further complicated when consideration is given to the fact that the global climate system is extremely complex, and therefore, climate time series must be expected to be nonstationary and nonlinear (Wu et al., 2007).

The objective of this paper is to examine the historical behavior of precipitation at CDMX and its possible relation to AMO by means of nonlinear techniques, which permit the extraction of cycles and secular trends from the data (Wu et al., 2011). Such extracted nonlinear trends are not constrained to follow a prescribed shape while allowing variation with time after the intrinsic variability at multidecadal and shorter timescales is suppressed. These nonlinear trends have a low sensitivity to the addition of new data, since new data in the future cannot alter the past tendency, a property that physical systems must have in their time evolution (see Ji et al., 2014, and references therein).

2. Data and Methods

In this study we use monthly averages of SST data and both observational and reanalysis precipitation data sets to generate time series of yearly averaged SSTs and annual accumulated precipitation.

2.1. Observational and Reanalysis Precipitation Data

Given the significant differences in precipitation estimates by the currently available data sets (Gehne et al., 2016), we use different sources of information regarding precipitation rates at several timescales. Thus, this study relies on the following data sets. Daily precipitation data recorded at Tacubaya station in CDMX for the period January 1877 to June 2017, provided by the Mexican National Weather Service. The National Aeronautics and Space Administration Tropical Rainfall Measuring Mission (TRMM) Multi-Satellite Precipitation Analysis (versions 6 and 7) that combines both infrared and passive microwave sensors to estimate precipitation in near real time (Huffman et al., 2007). In order to analyze monthly fields, we use the 3B4 precipitation product, downloaded from https://disc2.gesdisc.eosdis.nasa.gov/data/TRMM_L3/TRMM_3B43.7/. Additionally, the CPC Global Unified Precipitation data provided by the NOAA/OAR/ESRL PSD, Boulder, Colorado, USA, from their web site at http://www.esrl.noaa.gov/psd/is used. Three more precipitation data sets are considered here: Climate Hazards group Infrared Precipitation with Stations (CHIRPS; Funk et al., 2015), Livneh data set (Livneh et al., 2015), and Climate Prediction Center Morphing Technique (CMORPH; Joyce et al., 2004).

We complement our study of the precipitation trends in the CDMX region with data from three reanalysis systems: the ERA-Interim precipitation data provided by the European Centre for Medium Range Weather Forecast (Dee et al., 2011), the Modern-Era Retrospective Analysis for Research and Applications, version 2 (MERRA-2, Gelaro et al., 2017), and the National Centers for Environmental Prediction–National Center for Atmospheric Research (NCEP–NCAR) global reanalysis (Kalnay et al., 1996).

2.2. SST Data

In order to link precipitation trends to the state of the ocean, we use monthly SSTs fields from the Met Office Hadley Centre's sea ice and SST (HadISST) data set version 1.1, which is an interpolated SST data set, with 1° × 1° spatial resolution, covering the period from 1870 to present (Rayner et al., 2003). For the study of the impact of North Atlantic SST on the year-to-year variability of precipitation over CDMX, we use yearly averages of the monthly values of SSTs averaged in the box 75.5°W to 6.5°W, 24.5°N to 60.5°N. The resulting time series are representative of the North Atlantic and will be simply referred to as yearly SST.

2.3. Nonlinear Decomposition of Time Series

In order to separate time series in its different frequency and amplitude components, we use state-of-the-art Ensemble Empirical Mode Decomposition (EEMD) method, which, as stated by Wu and Huang (2009) and explained below, represents a major improvement over the EMD method. In brief, the EMD method permits the partition, via a sifting process, of nonstationary and nonlinear signals contained in a time series into a set of intrinsic mode function components (IMFs; Huang et al., 1998). At each step of the sifting process, an oscillatory component is extracted from the original time series, with the first IMF corresponding to the highest-frequency oscillation, and so on (Wu et al., 2007). Once all the oscillatory components are extracted, the residual, which is either a monotonic function or has only one extremum, is identified as the trend. In the EEMD method, an ensemble is generated by adding white noise to the original signal; thus, the sifting process is performed over this ensemble, considering the mean as the final end result of this process (Wu & Huang, 2009). The added noise to the signal in the EEMD method is an important improvement over the EMD method. Indeed, as Wu and Huang (2009) show, by adding white noise (with an appropriate amplitude) to the original time series, it is possible to identify that part of the signal that scales similarly in magnitude as the IMF of interest, thus avoiding the need to introduce an a priori criterion as is usually done in the tests of intermittency in the previous EMD technique. Wu and Huang (2009) suggested "to add noise of an amplitude that is about 0.2 standard deviation of that of the data. However, when the data is dominated by high-frequency signals, the noise amplitude may be smaller, and when the data is dominated by low-frequency signals, the noise amplitude may be increased." We used different noise amplitudes, with values ranging from 0.2 to 0.4, obtaining similar results. In all decompositions reported here, noise of standard deviation 0.35 is added to the target data for the ensemble calculation, and an ensemble number of 1,000 is used.

Another very important feature of the EEMD algorithm is the fact that new data in the future does not alter the past tendency. As stated in Ji et al. (2014), "the extracted trend follows no a priori shape and varies with time after the intrinsic variability of multi-decadal and shorter timescales is removed. This trend also has low sensitivity to the extension (addition) of new data. This property guarantees that the physical interpretation within specified time intervals does not change with the addition of new data, consistent with a physical constraint that the subsequent evolution of a physical system cannot alter the reality that has already happened."

The constructed yearly time series of SST and accumulated precipitation are both decomposed using EEMD. As stated by Ji et al. (2014), "a time series at a grid point x (t) is decomposed using EEMD in terms of adaptively obtained, amplitude-frequency modulated oscillatory components C_j (j = 1, 2, …, n) and a residual R_n, a curve either monotonic or containing only one extremum from which no additional oscillatory components can be extracted:

$$x(\mathrm{t}) = \sum_{j=1}^{n} C_j(\mathrm{t}) + \mathrm{R}_n(\mathrm{t}),\text{"}$$

where x (t) denotes either yearly time series of precipitation or SST; each C_j (t), the jth extracted oscillatory component of precipitation or SST; and R_n, the secular trend, hereafter referred as the trend. The significance of all extracted oscillatory components was tested against the null hypothesis of climate noise following the work of Franzke (2009). This methodology, however, was not designed for testing the significance of the secular trends. Ji et al. (2014) proposed a novel approach to determine the statistical significance of secular trends using a Monte Carlo method, which we applied in this work.

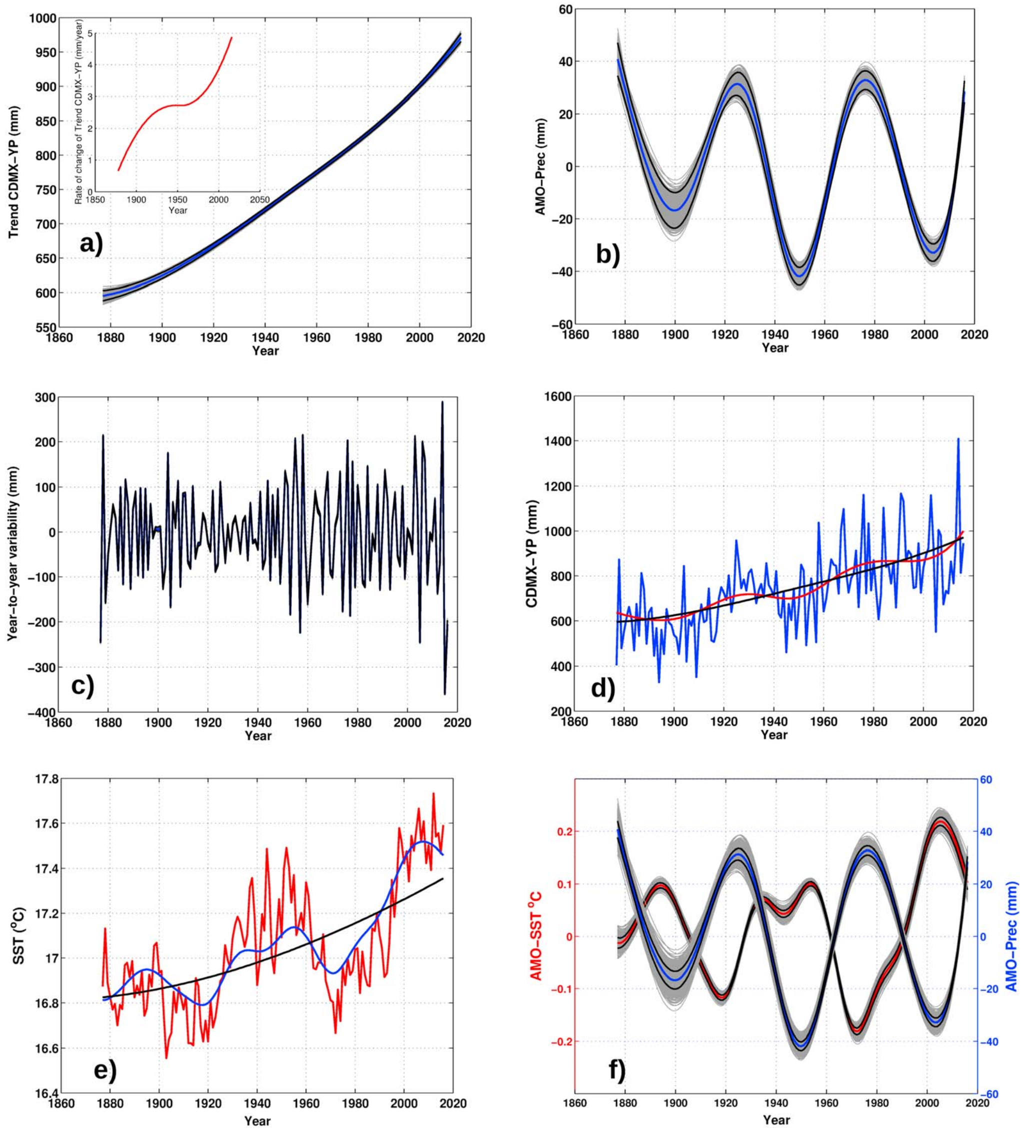

Figure 1. (a) Secular trend. The inset shows the rate of change of the mean secular trend of precipitation. The gray lines are the precipitation trends extracted from 1,000 realizations of the noise-added CDMX-YP time series. Mean secular trend of precipitation (ensemble mean, blue line). Black lines correspond to two standard deviations that are used here as a confidence interval for the 1,000 secular trends. Panels (b) and (c) are the same as (a) but for both AMO-related and year-to-year precipitation variability, respectively. (d) Reconstructed CDMX-YP time series by using all modes derived from the Ensemble Empirical Mode Decomposition, which is equal to the original precipitation series (blue line). The secular trend and the reconstruction using only the secular trend and the AMO-related variability are indicated by the black and red line, respectively. (e) Mean secular trend of SST, mean AMO-related SST variability, and reconstructed yearly SST series from the Ensemble Empirical Mode Decomposition (black, blue, and red lines, respectively). (f) AMO-related variability for both CDMX-YP and yearly SST. The gray lines are the AMO-related values for both yearly SST and CDMX-YP extracted from 1,000 realizations of the noise-added yearly SST and CDMX-YP time series. Ensemble mean for CDMX-YP (blue line) and yearly SST (red line). Black lines correspond to two standard deviations. AMO = Atlantic Multidecadal Oscillation; CDMX-YP = annual precipitation time series at Mexico City; SST = sea surface temperature.

3. Decomposition of Annual Precipitation

3.1. Secular Trends

The annual precipitation time series at CDMX (hereafter denoted as CDMX-YP) was decomposed using the EEMD method. Figure 1a shows the mean CDMX-YP secular trend. Since 1877, the CDMX-YP has increased by roughly 63%. The yearly rate of increase in rainfall, however, has not been uniform throughout the record (see red line from inset). During the first decade of the record, the mean year-to-year increase was of about 1 mm/year, reaching slightly more than 2 mm/year during the first decade of the twentieth century. Then, approximately from 1940 to 1960 the increase was linear (about 2.7 mm/year), accelerating from 1961 onward and reaching a value of about 4.5 mm/year during the last decade. The beginning of this accelerated increase of annual precipitation coincides with the time when a significant growth was registered during the 1960s in CDMX (Jauregui & Romales, 1996); thus, the accelerated increase of annual precipitation from 1961 could be related to the accelerated urban growth (see next paragraph). The statistical significance of secular trends was tested using a Monte Carlo method (Ji et al., 2014). According to this methodology, our trends were statistically significant at above the 95% confidence level (see Figure S1 in the supporting information).

In addition to the urban-induced effect on precipitation, a second man-induced effect is global warming, which has contributed to the observed precipitation trend in many regions around the world in the last decades (e.g., Armal et al., 2018; Parr et al., 2015; Zhou et al., 2017). It is a difficult task to distinguish between both global warming and urban-induced contributions to the observed trend in precipitation, as the sources of observational coverage remain sparse, particularly in the tropics. To the best of our knowledge, few studies have focused on this topic in Mexico. One first attempt, however, is the work of Jauregui and Romales (1996), who analyzed rainfall data for both urban and suburban stations for the period 1941–1985. They showed that a suburban station (located in the northeast part of the CDMX, away from high-density building) does not show any trend, while an urban station located in the west part of the CDMX displays a significant increase during the analyzed period. It is well known that urban heat islands are responsible for greater horizontal temperature gradients between rural vegetated surfaces and urbanized built areas. These temperature gradients are, in turn, the result of different energy partitions from the different land use and land cover that characterize this particular catchment basin. Typically, during the diurnal cycle, urban areas can display larger turbulent sensible heat fluxes than those of rural areas and forested areas over mountain slopes. Thus, it is expected that at the center and at the edge of the urban heat islands larger vertical velocities be induced. Thus, under the right atmospheric instability conditions (with local and remotely provided water vapor sources) this is conducive to the formation of deep convection and precipitation later in the day (Ochoa et al., 2015). Thus, it seems reasonable to assume that the increase in precipitation registered at Tacubaya over that period is somehow connected to urban growth (Ochoa et al., 2015); this, however, does not rule out that global warming nor other sources of low-frequency variability like wet-dry anomalies of the past (Lachniet et al., 2017) are possible contributors to this trend as well.

The observed secular positive trend in precipitation for the CDMX, however, can be also thought of as part of a long-term, natural oscillation. In fact, several long-term wet and dry anomalies have already occurred. For example, between −13 and 191 CE, the strongest wet anomaly of the last two millennia was registered, which had a duration of 205 years in a period known as the Teotihuacan pluvial, followed by a dry period of 33 years (191 to 223 CE). More than a millennia later, a second strongest wet anomaly occurred with a duration of 179 years, between 1317 and 1495 CE, period known as the Aztec pluvial, which was followed by a dry period of 65 years (1495 to 1559 CE) known as the Conquest interpluvial (Lachniet et al., 2017). Currently, the CDMX precipitation trend is consistent with this paleoclimatic upward trend in precipitation according to Lachniet et al. (2017). Due to the limited length and scarcity of the precipitation time series it is only possible to extract part of the oscillation, in other words, a positive anomaly with respect to a sufficiently long period. In this manner, we have to consider the observed trends in precipitation as the combination of man-made forcing and a natural one. It is not clear whether a dry period can occur after the end of the present wet anomaly, or how the global warming could affect the future behavior of precipitation at CDMX; however, on the basis of the past evidence presented by Lachniet et al. (2017), a dry period lasting several decades, or even longer, is a possibility that cannot be ruled out a priori.

Finally, to find out whether the trend in precipitation is distributed uniformly over the year we analyzed the trends of the monthly precipitation series. These results show that the wet season (May to October) has positive, statistically significant trends, while the dry months (November to April) exhibit no variation in their values (figures not shown).

3.2. Oscillatory Components of Precipitation and their Relation to AMO and Year-to-Year Variability

Although our analysis clearly detected trends in annual precipitation, the contribution of these trends coming from anthropogenic activities is hard to determine, particularly at local and regional levels due to the large observed precipitation variability at these scales, which includes both natural and forced variability. In order to estimate the contribution of multidecadal variability to the total variance, we analyzed the multidecadal variability extracted from the precipitation series. Figure 1b shows the mean AMO-related variability mode for precipitation (hereafter the adjective *mean* is omitted), which has time-dependent amplitude with values ranging from about −40 to +30 mm, representing a maximum contribution of about 70 mm to the observed annual precipitation in a time period of approximately 25 years. In contrast, the contribution of year-to-year variability (Figure 1c) to the annual precipitation is much larger, with both positive and negative values sometimes increasing (or decreasing) the annual precipitation in more than 600 mm in 1 year. A visual inspection of the whole precipitation time series and the reconstructed one using the trend plus the AMO-related variability (Figure 1d) reveals the huge contribution of the high-frequency variability to the annual precipitation. Note that we used the term AMO-related variability to indicate multidecadal variability with a timescale similar to that of the AMO. The mean AMO-related variability indicates the fact that we obtain an ensemble of 1,000 members by adding at each iteration an independent realization of white noise to the target data and then extracting the modes. Thus, we obtained six modes by averaging this ensemble, and the fourth mode corresponds to the multidecadal variability similar to that of the AMO. As already indicated, the adjective mean is hereafter omitted.

To detect any relationship between the precipitation variability at CDMX and the SST variability in the tropical North Atlantic SST, we compared the low-frequency modes resulting from the decomposition of yearly SSTs over that oceanic region with the corresponding low-frequency precipitation modes. Figure 1e shows the mean secular trend, the mean AMO-related variability, and the reconstructed yearly SST series. Figure 1f shows the mean AMO-related variability for both precipitation and yearly SSTs. A clear negative overall correlation between the AMO-related variability of SST and CDMX-YP is evident (−0.72 for the whole period 1877–2016): when AMO is positive (warm phase), annual accumulated precipitation tends to decrease and conversely in the cold phase of AMO. This correlation increases to −0.90 for the period 1960–2016. Note that the increment in correlation in this shorter period is related to the lack of the two peaks in SST found in the longer period from 1930 to 1960 that have no counterpart in the AMO-related precipitation mode. An open question is to identify the physical mechanisms involved in the coherent variation of yearly SST and annual precipitation at multidecadal timescales. This topic clearly deserves a further deeper analysis, which will be reported elsewhere.

So far, our results indicate that variability of rainfall in Tacubaya is largely due to three contributions: a sustained secular trend, a multidecadal oscillation highly correlated with AMO, and year-to-year variability, with the latter being the largest contributor. None of our extracted oscillatory components was statistically significant with respect to red noise. In particular, this was the case for the AMO-related variability of both precipitation and SST (see Franzke, 2009 for a description of this significance test). Similar results were obtained by using the significance test introduced by Wu et al. (2011) to determine the significance level of the multidecadal oscillatory component extracted by EEMD against a red noise null hypothesis.

To this day, a general consensus regarding what physical processes are involved in the evolution of the AMO is lacking. In the past, it has been related to the heat transport variability induced by the Atlantic Meridional Overturning Circulation (Delworth et al., 2007; Deser et al., 2010; Knight et al., 2005). Recently, Clement et al. (2015) proposed that "the AMO is the response to stochastic forcing from the mid-latitude atmospheric circulation, with thermal coupling playing a role in the tropics. In this view, the AMOC and other ocean circulation changes would be largely a response to, not a cause of, the AMO," which is consistent with our results, in the above-mentioned sense. This motivated us to use a simplified box model of the atmosphere-ocean system with diffusion (Wigley & Schlesinger, 1985), and driven by noise, to explore if this quite simple model is able to generate multidecadal variability consistent with the observed one. In this model, the upper ocean is represented by a mixed layer with constant depth, evolving in time in response to variations in the surface thermal forcing, atmospheric feedback, and energy transfer from the upper ocean to the deeper diffusive ocean. A description of this model is given in the book of McGuffie and Henderson-Sellers (2005).

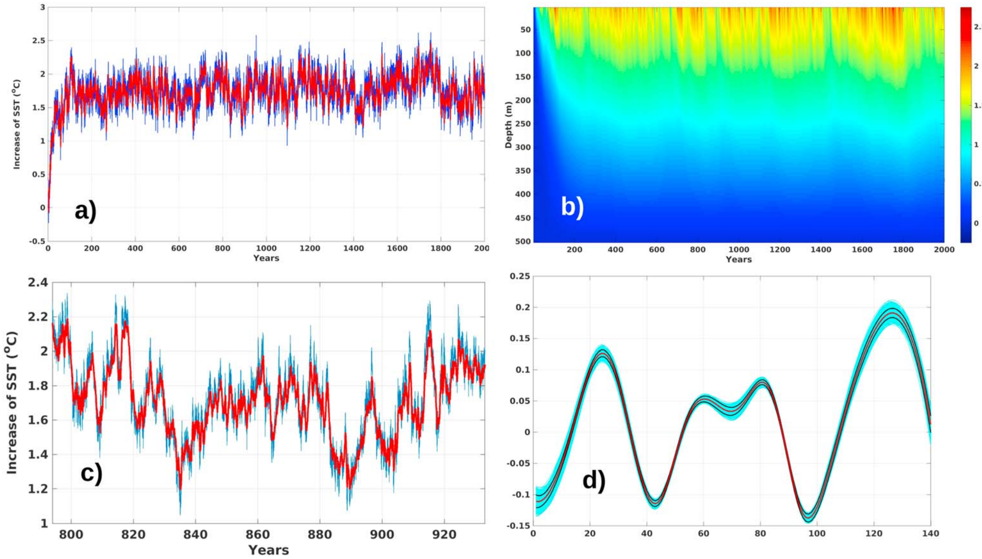

Figure 2. Results of a simple box model of the atmosphere-ocean system with a diffusive ocean (Wigley & Schlesinger, 1985) forced by a constant heat flux (Q = 4 W/m^2) and an additional white noise term to generate time series of yearly SST for a period of 2,000 years. Evolution of both SST (a) and the vertical profile of increase of temperature (b). We analyzed time intervals of 140 years and, in one of them (c), the extracted multidecadal oscillatory component (d) is quite similar to the AMO-related variability shown in Figures 1e and 1f. The depth of the mixed layer of the ocean was 100 m, which is coupled to a diffusive deep ocean (500 m thick), with a diffusion coefficient of 1×10^{-5} m^2/s. Notice that the amplitude of the long-term SST variability (a–c) is independent of the constant heat flux; indeed, it is centered about 0 if Q = 0, but the AMO-like variability remains unchanged (d). In (d), the cyan lines are 1,000 realizations of the noise-added yearly SST series generated by the model. The red line depicts the mean of the ensemble and the black lines correspond to two standard deviations.

In our experiments, the mixed layer is forced by a constant heat flux plus a white noise component to generate yearly SST time series for an interval of 2,000 years (see Figures 2a and 2b). We analyzed time intervals of 140 years within the 2,000-year period and found that in one of them (Figure 2c), the extracted multidecadal oscillatory component (Figure 2d) was quite similar to the AMO-related variability shown in Figures 1e and 1f. This result indicates that a quite simple model of the atmosphere-ocean system, forced by white noise, is capable to produce AMO-like SST variability that is entirely consistent with observations, supporting the findings of Clement et al. (2015). So far, our results indicate that the observed AMO-related variability of both SST and precipitation is undistinguishable from a red noise process. On the other hand, a quite simple model is capable of producing a similar kind of SST variability when forced with white noise. This suggests that the null hypothesis of Hasselmann (1976), whereby the reddening of the temperature spectrum is the result of integrating weather noise through the thermal inertia of the surface ocean represented here by a bulk mixed layer model, can be used to explain the observed temporal pattern of long-term AMO-related SST variability. How this long-term pattern of weather noise-induced ocean variability can modulate the long-term precipitation variability is an open question that deserves a further deeper analysis, which will be reported elsewhere.

Although the highest-frequency IMF is indistinguishable from red noise, it deserves a careful analysis. The precipitation volatility (year-to-year variation of annual accumulated precipitation) shows an increase in 2014 (Figures 1c and 1d). In fact, the maximum value of annual accumulated precipitation for the entire period is 1,408 mm in 2014, with June making the largest contribution to it (102 mm). The maximum of monthly precipitation, however, corresponds precisely to June 1968 (141 mm), with June's 1964, 1991, and 2014 having the next highest values (105, 103, and 102 mm, respectively). An examination of the precipitation daily values in Tacubaya indicated that only on 23 June 2014, it rained 76 mm, roughly 54% of the highest monthly maximum precipitation amount registered in 141 years. An analysis of infrared GOES-13 images (Knapp, 2008) showed a fast development of a large low pressure zone located over the abnormally warm waters of the Mexican Pacific off the mouth of the Gulf of California, inducing advection of warm moist air from the Pacific toward Central Mexico (see Figure S2 in the supporting information). This warm moisture flow

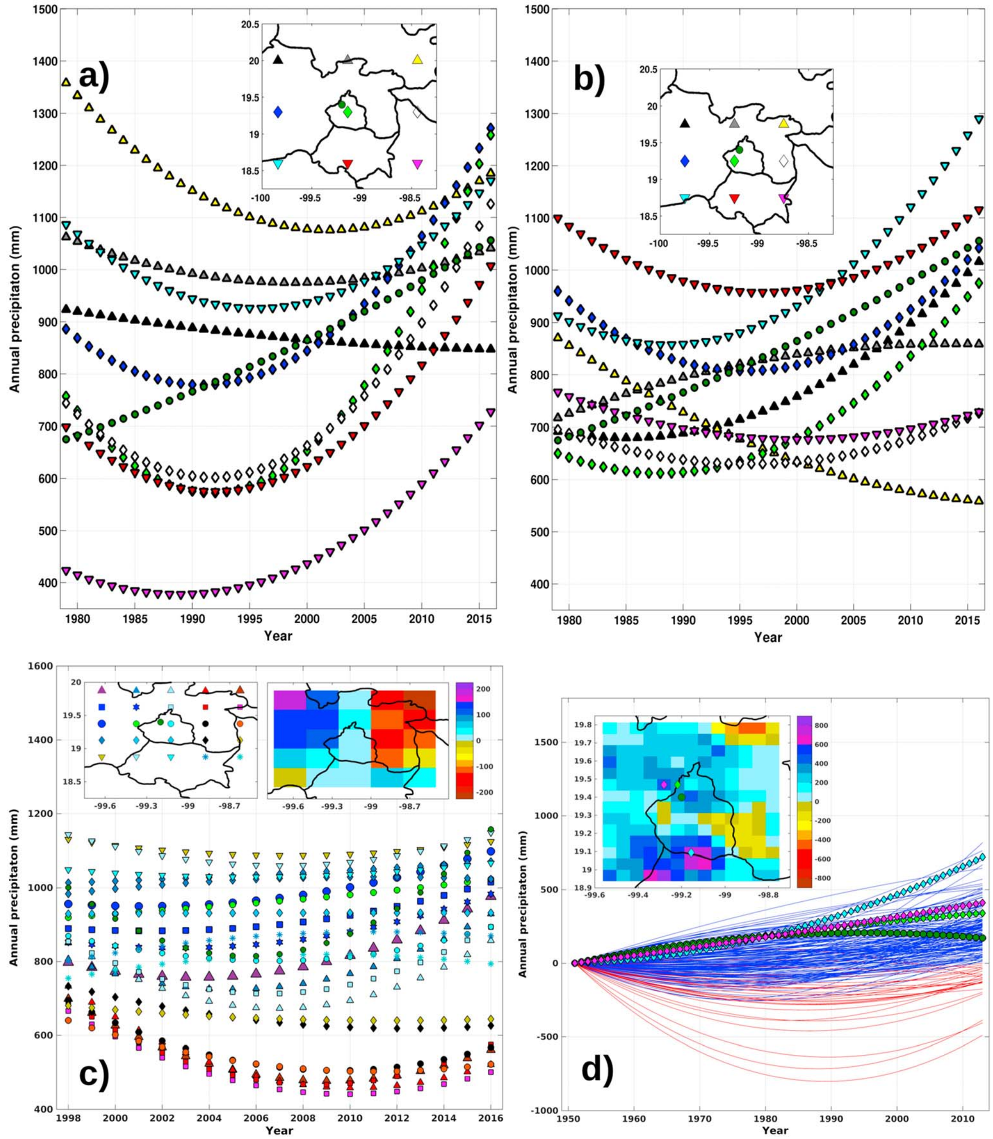

Figure 3. Mean secular precipitation trends extracted from ERA Interim reanalysis (a), Climate Prediction Center data (b), Tropical Rainfall Measuring Mission data (c), and Livneh data (d). The dark green circles show trends extracted from Tacubaya's observations for the corresponding analyzed periods. The colored patterns in (c) and (d) show the differences between end and initial values of the annual mean precipitation time series (2016 minus 1998 and 2013 minus 1951, respectively; unit: mm). Therefore, positive values (light-blue-to-purple colors) indicate increase in precipitation, while negative values (straw yellow-to-red colors) indicate decrease in precipitation. Blue and red solid lines in (d) show, respectively, the positive and negative precipitation trends at each location of the colored pattern. The largest decreases occur northeast from Mexico City.

interacted with an additional moisture flow coming from the Gulf of Mexico, thus favoring the development of a well-defined convection area in eastern Central Mexico and yielding, some hours later, a vast region of enhanced convection and heavy precipitation in CDMX. Clearly, the nature of such extreme hydrometeorological events is random; however, there is an intense debate about whether their increase, registered across the world, is caused by global warming (see, e.g., Coumou & Rahmstorf, 2012; Fischer & Knutti, 2014, 2015; Scherrer et al., 2016). Our results suggest an increase in the volatility of the annual accumulated precipitation (see Figure 1c), but an analysis of monthly values shows that the June's values, which is the month contributing the most to that increase, did not present such behavior. Hence, it is not evident if the weak increase of volatility in annual accumulated precipitation registered at CDMX is related to random events or that it does represent an initial stage of a period of increasing volatility associated with the global warming. Our analysis,

10.1029/2018EA000395

however, illustrates how high-frequency EEMD modes could be used to attribute some extreme events to one specific cause.

4. Observed and Simulated Precipitation at CDMX and Surrounding Areas for the Satellite Period

In this section we show how the generalized perception of increasing precipitation at several regions within CDMX and surrounding areas is supported by precipitation trends obtained from several reanalysis, precipitation, and satellite data sets.

Figure 3a shows several data points from ERA Interim reanalysis, chosen over a region that surrounds Mexico City. Starting in the 1990s, positive trends are evident in most of the data points. The observed nonlinear trend in Tacubaya (dark green circles) and the corresponding trend from the nearest point in the reanalysis (light green rhomboids) are comparable in magnitude but not in their time evolution. Note that from 1979 until 1990 most of the reanalysis points show a negative trend. We note, however, that NCEP and MERRA-2 reanalysis data points do not match this behavior (see Figures S3a and S3b in the supporting information).

CPC data points (Figure 3b), however, show negative trends from 1979 until about 1988. After 1988, CPC trends match that of Tacubaya, excepting one in Morelos and two in the State of Mexico. This increase in precipitation is also present in both TRMM and Livneh data (Figures 3c and 3d), although there are some clear differences between them. In particular, TRMM data show the largest increase in precipitation in the area located northwestward of CDMX. Livneh data are consistent with this area of positive trends (magenta circles in Figure 3d), but the largest increases occur in the south, over the border mountain region between CDMX and Morelos State (blue circles in Figure 3d). Notice that the analyzed period of Livneh data is longer than that of TRMM; however, since 1990s a generalized increase in precipitation is evident in both Livneh and TRMM data, in agreement with ERA Interim and CPC data.

Finally, CHIRPS data show a weak increase of precipitation in locations close to Tacubaya, and decreasing values elsewhere, while CMORPH data show an overall decreasing precipitation field (see Figures S3c and S3d in the supporting information). It is not clear why the extracted nonlinear trends from CHIRPS and CMORPH data in Central Mexico are so different of those extracted from TRMM and Livneh data. On the basis of Tacubaya, Livneh, CPC, and TRMM data sets, as well as on the basis of ERA Interim, NCEP, and MERRA-2, however, it seems reasonable to assume that the observed long-term precipitation trend in Tacubaya is not an isolated phenomenon but it is part of a wet anomaly covering a large part of CDMX and surrounding areas.

5. Summary

Nonlinear decomposition of yearly accumulated precipitation data shows that the variability of precipitation in Tacubaya is largely due to three contributions: a long-term secular positive trend, a multidecadal oscillation highly correlated with AMO, and year-to-year variability, with the latter being the largest contributor.

Average positive trends of about 4 mm/year for precipitation for the last 63 years (1951–2013) using climate historical data (Livneh et al., 2015) and about 3.6 mm/year for the last 19 years using TRMM data (1998–2016) were obtained using the EEMD technique for Central Mexico. Furthermore, the analysis of the longest record of historical precipitation data at Tacubaya station with the EEMD algorithm shows that this positive trend can be found as far back as the end of the nineteenth century and constitute a longer secular trend of about 360 mm in the last 140 years. Jauregui and Romales (1996) and Ochoa et al. (2015) suggest that land use land cover change might be contributors to the observed secular trends in precipitation over the CDMX. A larger heat island effect as a result of an accelerated urbanization could explain the observed increase in precipitation since the 1940s. Global warming, on the other hand, would increase the amount of water vapor available in the atmosphere leading to a change in hydrological cycle (Held & Soden, 2006) with the wet gets wetter and dry gets drier scenario. This possible behavior is still a matter of controversy (Greve & Seneviratne, 2015) and a difficult result yet to establish for Central Mexico. Recently, Lachniet et al. (2017) showed that the CDMX basin has been subjected to a series of alternating wet and dry periods for the last 2,000 years. Their results show paleoclimatic proxy data to match historical precipitation data at Tacubaya. We speculate that this kind of natural long-term variations in precipitation could contribute to the observed trends in precipitation and could be considered a possible driving mechanism.

It is not known how global warming could affect the future behavior of precipitation at CDMX, or how long our city will still receive large amounts of precipitation, but considering past evidence, a dry period lasting several decades, or even longer, is a possibility that should be carefully analyzed in order to define long-term water policy to overcome future social problems in CDMX related with an important deficit in water supply. Our best incentive to act is the current emergency situation in Cape Town, which can become in the next months the first major global city losing its piped potable water supply due to the worst drought to hit South Africa in almost a century.

The AMO-related variability of both precipitation and SST were not statistically significant with respect to red noise, and this motivated us to use a quite simplified box model of the atmosphere-ocean system with diffusion, forced by white noise, to generate time series of yearly SST. This simple model produced AMO-like variability that was entirely consistent with that obtained from the observations. This result is relevant because it implies that at multidecadal timescales, the SST variability in the North Atlantic is consistent with the stochastic climate model introduced by Hasselmann (1976) and by Frankignoul and Hasselmann (1977); in other words, the integrated response of the oceanic surface layers to short timescale atmospheric forcing may be sufficient to naturally explain observed SST variability at multidecadal timescales in the North Atlantic without resorting to deterministic external forcing or ocean dynamical modes, as is usually done in the literature.

Acknowledgments
We would like to acknowledge partial financial support from "Programa de Apoyo a Proyectos de Investigación e Innovación Tecnológica (PAPIIT IA100912), UNAM" and from the project "Pronóstico estacional de condiciones de sequía meteorológica en México utilizando un sistema de modelación climática regional para el desarrollo de un prototipo de sistema de alerta por sequía" funding by CENAPRED. We thank to O. Cervántes Sánchez (Comisión Nacional del Agua, CONAGUA, México) for providing us with the Tacubaya precipitation data. We also thank the state assignment of FASO Russia (theme 0149-2018-0014). Finally, we would like to thank the reviewers for their constructive comments.

References

Alexander, M. A., Kilbourne, K. H., & Nye, J. A. (2014). Climate variability during warm and cold phases of the Atlantic Multidecadal Oscillation (AMO) 1871–2008. *Journal of Marine Systems*, *133*, 14–26. https://doi.org/10.1016/j.jmarsys.2013.07.017

Allan, R. P., & Soden, B. J. (2008). Atmospheric warming and the amplification of precipitation extremes. *Science*, *321*(5895), 1481–1484. https://doi.org/10.1126/science.1160787

Armal, S., Devineni, N., & Khanbilvardi, R. (2018). Trends in extreme rainfall frequency in the contiguous United States: Attribution to climate change and climate variability modes. *Journal of Climate*, *31*(1), 369–385. https://doi.org/10.1175/JCLI-D-17-0106.1

Castro, C. L., McKee, T. B., & Pielke, R. A. Sr. (2001). The relationship of the North American monsoon to tropical and North Pacific sea surface temperatures as revealed by observational analyses. *Journal of Climate*, *14*(24), 4449–4473. https://doi.org/10.1175/1520-0442(2001)014<4449:TROTNA>2.0.CO;2

Clement, A., Bellomo, K., Murphy, L. N., Cane, M. A., Mauritsen, T., Rädel, G., & Stevens, B. (2015). The Atlantic Multidecadal Oscillation without a role for ocean circulation. *Science*, *350*(6258), 320–324. https://doi.org/10.1126/science.aab3980

Coumou, D., & Rahmstorf, S. (2012). A decade of weather extremes. *Nature Climate Change*, *2*(7), 491–496. https://doi.org/10.1038/nclimate1452

Curtis, S. (2008). The Atlantic multidecadal oscillation and extreme daily precipitation over the US and Mexico during the hurricane season. *Climate Dynamics*, *30*(4), 343–351. https://doi.org/10.1007/s00382-007-0295-0

Dee, D. P., Uppala, S. M., Simmons, A. J., Berrisford, P., Poli, P., Kobayashi, S., et al. (2011). The ERA-Interim reanalysis: Configuration and performance of the data assimilation system. *Quarterly Journal of the Royal Meteorological Society*, *137*(656), 553–597. https://doi.org/10.1002/qj.828

Delworth, T. L., Zhang, R., & Mann, M. E. (2007). Decadal to centennial variability of the Atlantic from observations and models. In *Ocean circulation: Mechanisms and impacts—Past and future changes of meridional overturning* (pp. 131–148). Washington, DC: American Geophysical Union.

Deser, C., Alexander, M. A., Xie, S.-P., & Phillips, A. S. (2010). Sea surface temperature variability: Patterns and mechanisms. *Annual Review of Marine Science*, *2*(1), 115–143. https://doi.org/10.1146/annurev-marine-120408-151453

Donat, M. G., Lowry, A. L., Alexander, L. V., O'Gorman, P. A., & Maher, N. (2016). More extreme precipitation in the world's dry and wet regions. *Nature Climate Change*, *6*(5), 508–513. https://doi.org/10.1038/nclimate2941

Easterling, D. R., Meehl, G. A., Parmesan, C., Changnon, S. A., Karl, T. R., & Mearns, L. O. (2000). Climate extremes: Observations, modeling, and impacts. *Science*, *289*(5487), 2068–2074.

Enfield, D. B., Mestas-Nuñez, A. M., & Trimble, P. J. (2001). The Atlantic multidecadal oscillation and its relation to rainfall and river flows in the continental US. *Geophysical Research Letters*, *28*(10), 2077–2080. https://doi.org/10.1029/2000GL012745

Fischer, E. M., & Knutti, R. (2014). Detection of spatially aggregated changes in temperature and precipitation extremes. *Geophysical Research Letters*, *41*, 547–554. https://doi.org/10.1002/2013GL058499

Fischer, E. M., & Knutti, R. (2015). Anthropogenic contribution to global occurrence of heavy-precipitation and high-temperature extremes. *Nature Climate Change*, *5*(6), 560–564. https://doi.org/10.1038/nclimate2617

Frankignoul, C., & Hasselmann, K. (1977). Stochastic climate models, Part II Application to sea-surface temperature anomalies and thermocline variability. *Tellus*, *29*(4), 289–305.

Franzke, C. (2009). Multi-scale analysis of teleconnection indices: Climate noise and nonlinear trend analysis. *Nonlinear Processes in Geophysics*, *16*(1), 65–76. https://doi.org/10.5194/npg-16-65-2009

Funk, C., Peterson, P., Landsfeld, M., Pedreros, D., Verdin, J., Shukla, S., et al. (2015). The climate hazards infrared precipitation with stations—a new environmental record for monitoring extremes. *Scientific Data*, *2*, 150066

Gehne, M., Hamill, T. M., Kiladis, G. N., & Trenberth, K. E. (2016). Comparison of global precipitation estimates across a range of temporal and spatial scales. *Journal of Climate*, *29*(21), 7773–7795. https://doi.org/10.1175/JCLI-D-15-0618.1

Gelaro, R., McCarty, W., Suárez, M. J., Todling, R., Molod, A., Takacs, L., et al. (2017). The modern-era retrospective analysis for research and applications, version 2 (MERRA-2). *Journal of Climate*, *30*(14), 5419–5454. https://doi.org/10.1175/JCLI-D-16-0758.1

Greve, P., & Seneviratne, S. I. (2015). Assessment of future changes in water availability and aridity. *Geophysical Research Letters*, *42*, 5493–5499. https://doi.org/10.1002/2015GL064127

Hasselmann, K. (1976). Stochastic climate models Part I. Theory. *Tellus*, *28*(6), 473–485.

Held, I. M., & Soden, B. J. (2006). Robust responses of the hydrological cycle to global warming. *Journal of Climate*, *19*(21), 5686–5699. https://doi.org/10.1175/JCLI3990.1

Higgins, R. W., Chen, Y., & Douglas, A. V. (1999). Interannual variability of the North American warm season precipitation regime. *Journal of Climate*, *12*(3), 653–680. https://doi.org/10.1175/1520-0442(1999)012<0653:IVOTNA>2.0.CO;2

Huang, N. E., Shen, Z., Long, S. R., Wu, M. C., Shih, H. H., Zheng, Q., et al. (1998). The empirical mode decomposition and the Hilbert spectrum for nonlinear and non-stationary time series analysis. *Proceedings of the Royal Society of London A: mathematical, physical and engineering sciences*, *454*(1971), 903–995. The Royal Society

Huffman, G. J., Bolvin, D. T., Nelkin, E. J., Wolff, D. B., Adler, R. F., Gu, G., et al. (2007). The TRMM multisatellite precipitation analysis (TMPA): Quasi-global, multiyear, combined-sensor precipitation estimates at fine scales. *Journal of Hydrometeorology*, *8*(1), 38–55. https://doi.org/10.1175/JHM560.1

IPCC (2013). Climate change 2013: The physical science basis. In T. F. Stocker, D. Qin, G.-K. Plattner, M. Tignor, S. K. Allen, J. Boschung, et al. (Eds.), *Contribution of Working Group I to the Fifth Assessment Report of the Intergovernmental Panel on Climate Change* (Chapter 9, p. 1535, pp. 760–762). Cambridge, United Kingdom and New York, NY, USA: Cambridge University Press. https://doi.org/10.1017/CBO9781107415324

Jauregui, E. (1973). The urban climate of Mexico City. *Erdkunde*, *27*, 298–307.

Jauregui, E., & Romales, E. (1996). Urban effects on convective precipitation in Mexico City. *Atmospheric Environment*, *30*(20), 3383–3389. https://doi.org/10.1016/1352-2310(96)00041-6

Ji, F., Wu, Z., Huang, J., & Chassignet, E. P. (2014). Evolution of land surface air temperature trend. *Nature Climate Change*, *4*(6), 462–466. https://doi.org/10.1038/nclimate2223

Joyce, R. J., Janowiak, J. E., Arkin, P. A., & Xie, P. (2004). CMORPH: A method that produces global precipitation estimates from passive microwave and infrared data at high spatial and temporal resolution. *Journal of Hydrometeorology*, *5*(3), 487–503. https://doi.org/10.1175/1525-7541(2004)005<0487:CAMTPG>2.0.CO;2

Kalnay, E., Kanamitsu, M., Kistler, R., Collins, W., Deaven, D., Gandin, L., et al. (1996). The NCEP/NCAR 40-year reanalysis project. *Bulletin of the American Meteorological Society*, *77*(3), 437–471. https://doi.org/10.1175/1520-0477(1996)077<0437:TNYRP>2.0.CO;2

Kerr, R. A. (2000). A North Atlantic climate pacemaker for the centuries. *Science*, *288*(5473), 1984–1985. https://doi.org/10.1126/science.288.5473.1984

Knapp, K. R. (2008). Scientific data stewardship of International Satellite Cloud Climatology Project B1 global geostationary observations. *Journal of Applied Remote Sensing*, *2*(1), 023548.

Knight, J. R. (2009). The Atlantic multidecadal oscillation inferred from the forced climate response in coupled general circulation models. *Journal of Climate*, *22*(7), 1610–1625. https://doi.org/10.1175/2008JCLI2628.1

Knight, J. R., Allan, R. J., Folland, C. K., Vellinga, M., & Mann, M. E. (2005). A signature of persistent natural thermohaline circulation cycles in observed climate. *Geophysical Research Letters*, *32*, L20708. https://doi.org/10.1029/2005GL024233

Kumar, S., Merwade, V., Kinter, J. L. III, & Niyogi, D. (2013). Evaluation of temperature and precipitation trends and long-term persistence in CMIP5 twentieth-century climate simulations. *Journal of Climate*, *26*(12), 4168–4185. https://doi.org/10.1175/JCLI-D-12-00259.1

Lachniet, M. S., Asmerom, Y., Polyak, V., & Bernal, J. P. (2017). Two millennia of Mesoamerican monsoon variability driven by Pacific and Atlantic synergistic forcing. *Quaternary Science Reviews*, *155*, 100–113. https://doi.org/10.1016/j.quascirev.2016.11.012

Latif, M. (2013). The ocean's role in modeling and predicting decadal climate variations. In *International geophysics* (Vol. 103, pp. 645–665). Oxford, UK: Academic Press.

Livneh, B., Bohn, T. J., Pierce, D. W., Munoz-Arriola, F., Nijssen, B., Vose, R., et al. (2015). A spatially comprehensive, hydrometeorological data set for Mexico, the US, and Southern Canada 1950–2013. *Scientific Data*, *2*, 150042.

McGuffie, K., & Henderson-Sellers, A. (2005). *A climate modelling primer* (3rd ed.). Chichester, UK: John Wiley.

Méndez, M., & Magaña, V. (2010). Regional aspects of prolonged meteorological droughts over Mexico and Central America. *Journal of Climate*, *23*(5), 1175–1188. https://doi.org/10.1175/2009JCLI3080.1

Ochoa, C. A., Quintanar, A. I., Raga, G. B., & Baumgardner, D. (2015). Changes in intense precipitation events in Mexico City. *Journal of Hydrometeorology*, *16*(4), 1804–1820. https://doi.org/10.1175/JHM-D-14-0081.1

Parr, D., Wang, G., & Ahmed, K. F. (2015). Hydrological changes in the US northeast using the Connecticut River basin as a case study: Part 2. Projections of the future. *Global and Planetary Change*, *133*, 167–175. https://doi.org/10.1016/j.gloplacha.2015.08.011

Pavia, E. G. (2009). The relationship between Pacific Decadal and Southern Oscillations: Implications for the climate of northwestern Baja California. *Geofísica internacional*, *48*(4), 385–389.

Pavia, E. G., Graef, F., & Fuentes-Franco, R. (2016). Recent ENSO–PDO precipitation relationships in the Mediterranean California border region. *Atmospheric Science Letters*, *17*(4), 280–285. https://doi.org/10.1002/asl.656

Pavia, E. G., Graef, F., & Reyes, J. (2006). PDO–ENSO effects in the climate of Mexico. *Journal of Climate*, *19*(24), 6433–6438. https://doi.org/10.1175/JCLI4045.1

Rayner, N. A., Parker, D. E., Horton, E. B., Folland, C. K., Alexander, L. V., Rowell, D. P., et al. (2003). Global analyses of sea surface temperature, sea ice, and night marine air temperature since the late nineteenth century. *Journal of Geophysical Research*, *108*(D14), 4407. https://doi.org/10.1029/2002JD002670

Santillán, N. S., López, R. G., Zepeda, R. V., & Trejo, R. S. (2012). Climate change in NE Mexico: Influence of the North Atlantic Oscillation. *Investigaciones geográficas*, (78), 7–18.

Scherrer, S. C., Fischer, E. M., Posselt, R., Liniger, M. A., Croci-Maspoli, M., & Knutti, R. (2016). Emerging trends in heavy precipitation and hot temperature extremes in Switzerland. *Journal of Geophysical Research: Atmospheres*, *121*, 2626–2637. https://doi.org/10.1002/2015JD024634

Schlesinger, M. E., & Ramankutty, N. (1994). An oscillation in the global climate system of period 65–70 years. *Nature*, *367*(6465), 723–726. https://doi.org/10.1038/367723a0

Sutton, R. T., & Hodson, D. L. (2005). Atlantic Ocean forcing of North American and European summer climate. *Science*, *309*(5731), 115–118. https://doi.org/10.1126/science.1109496

Taylor, K. E., Stouffer, R. J., & Meehl, G. A. (2012). An overview of CMIP5 and the experiment design. *Bulletin of the American Meteorological Society*, *93*(4), 485–498. https://doi.org/10.1175/BAMS-D-11-00094.1

Trenberth, K. E. (2011). Changes in precipitation with climate change. *Climate Research*, *47*(1/2), 123–138. https://doi.org/10.3354/cr00953

Westra, S., Fowler, H. J., Evans, J. P., Alexander, L. V., Berg, P., Johnson, F., et al. (2014). Future changes to the intensity and frequency of short-duration extreme rainfall. *Reviews of Geophysics*, *52*, 522–555. https://doi.org/10.1002/2014RG000464

Wigley, T. M., & Schlesinger, M. E. (1985). Analytical solution for the effect of increasing CO_2 on global mean temperature. *Nature*, *315*(6021), 649–652. https://doi.org/10.1038/315649a0

Wu, Z., & Huang, N. E. (2009). Ensemble empirical mode decomposition: A noise-assisted data analysis method. *Advances in Adaptive Data Analysis*, *01*(01), 1–41. https://doi.org/10.1142/S1793536909000047

Wu, Z., Huang, N. E., Long, S. R., & Peng, C. K. (2007). On the trend, detrending, and variability of nonlinear and nonstationary time series. *Proceedings of the National Academy of Sciences*, *104*(38), 14,889–14,894. https://doi.org/10.1073/pnas.0701020104

Wu, Z., Huang, N. E., Wallace, J. M., Smoliak, B. V., & Chen, X. (2011). On the time-varying trend in global-mean surface temperature. *Climate Dynamics*, *37*(3–4), 759–773. https://doi.org/10.1007/s00382-011-1128-8

Zhou, X., Bai, Z., & Yang, Y. (2017). Linking trends in urban extreme rainfall to urban flooding in China. *International Journal of Climatology*, *37*(13), 4586–4593. https://doi.org/10.1002/joc.5107